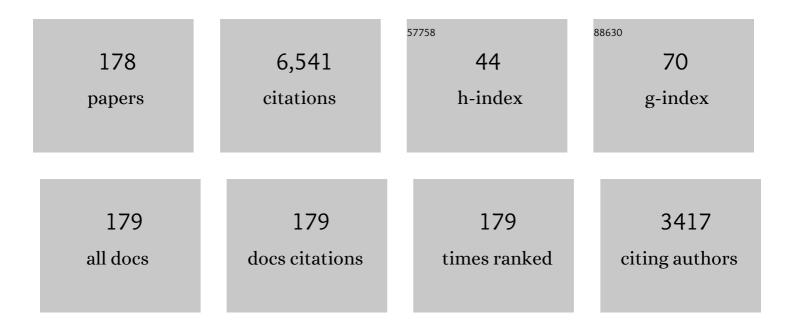
Mark A Clilverd

List of Publications by Year in descending order

Source: https://exaly.com/author-pdf/5931043/publications.pdf Version: 2024-02-01



#	Article	IF	CITATIONS
1	Examination of Radiation Belt Dynamics During Substorm Clusters: Activity Drivers and Dependencies of Trapped Flux Enhancements. Journal of Geophysical Research: Space Physics, 2022, 127, .	2.4	7
2	Geomagnetically Induced Current Model in New Zealand Across Multiple Disturbances: Validation and Extension to Nonâ€Monitored Transformers. Space Weather, 2022, 20, .	3.7	11
3	Role of hard X-ray emission in ionospheric D-layer disturbances during solar flares. Earth, Planets and Space, 2022, 74, .	2.5	3
4	HEPPA III Intercomparison Experiment on Electron Precipitation Impacts: 1. Estimated Ionization Rates During a Geomagnetic Active Period in April 2010. Journal of Geophysical Research: Space Physics, 2022, 127, .	2.4	16
5	Exceptional middle latitude electron precipitation detected by balloon observations: implications for atmospheric composition. Atmospheric Chemistry and Physics, 2022, 22, 6703-6716.	4.9	7
6	The Correspondence Between Sudden Commencements and Geomagnetically Induced Currents: Insights From New Zealand. Space Weather, 2022, 20, .	3.7	3
7	Geomagnetically induced currents during the 07–08 September 2017 disturbed period: a global perspective. Journal of Space Weather and Space Climate, 2021, 11, 33.	3.3	11
8	Lower-thermosphere–ionosphere (LTI) quantities: current status of measuring techniques and models. Annales Geophysicae, 2021, 39, 189-237.	1.6	25
9	Impact of EMICâ€Wave Driven Electron Precipitation on the Radiation Belts and the Atmosphere. Journal of Geophysical Research: Space Physics, 2021, 126, e2020JA028671.	2.4	4
10	Comparing Electron Precipitation Fluxes Calculated From Pitch Angle Diffusion Coefficients to LEO Satellite Observations. Journal of Geophysical Research: Space Physics, 2021, 126, e2020JA028410.	2.4	17
11	Quiet Night Arctic Ionospheric <i>D</i> Region Characteristics. Journal of Geophysical Research: Space Physics, 2021, 126, e2020JA029043.	2.4	4
12	Evidence of Subâ€MeV EMICâ€Driven Trapped Electron Flux Dropouts From GPS Observations. Geophysical Research Letters, 2021, 48, e2021GL092664.	4.0	5
13	Springâ€Fall Asymmetry in VLF Amplitudes Recorded in the North Atlantic Region: The Fallâ€Effect. Geophysical Research Letters, 2021, 48, e2021GL094581.	4.0	3
14	Impacts of UV Irradiance and Medium-Energy Electron Precipitation on the North Atlantic Oscillation during the 11-Year Solar Cycle. Atmosphere, 2021, 12, 1029.	2.3	3
15	Cross―Coherence of the Outer Radiation Belt During Storms and the Role of the Plasmapause. Journal of Geophysical Research: Space Physics, 2021, 126, e2021JA029308.	2.4	5
16	Solar flare Xâ€ray impacts on long subionospheric VLF paths. Space Weather, 2021, 19, e2021SW002820.	3.7	6
17	Ground-based very-low-frequency radio wave observations of energetic particle precipitation. , 2020, , 257-277.		1
18	Geomagnetically Induced Currents and Harmonic Distortion: High Time Resolution Case Studies. Space Weather, 2020, 18, e2020SW002594.	3.7	13

#	Article	IF	CITATIONS
19	Geomagnetically Induced Currents and Harmonic Distortion: Stormâ€Time Observations From New Zealand. Space Weather, 2020, 18, e2019SW002387.	3.7	19
20	Electron Precipitation From the Outer Radiation Belt During the St. Patrick's Day Storm 2015: Observations, Modeling, and Validation. Journal of Geophysical Research: Space Physics, 2020, 125, e2019JA027725.	2.4	9
21	Spatial Distributions of Nitric Oxide in the Antarctic Wintertime Middle Atmosphere During Geomagnetic Storms. Journal of Geophysical Research: Space Physics, 2020, 125, e2020JA027846.	2.4	3
22	A Multiâ€Instrument Approach to Determining the Sourceâ€Region Extent of EEPâ€Driving EMIC Waves. Geophysical Research Letters, 2020, 47, e2019GL086599.	4.0	10
23	Daedalus: a low-flying spacecraft for in situ exploration of the lower thermosphere–ionosphere. Geoscientific Instrumentation, Methods and Data Systems, 2020, 9, 153-191.	1.6	25
24	Magnetic Local Timeâ€Resolved Examination of Radiation Belt Dynamics during Highâ€Speed Solar Wind Speedâ€Triggered Substorm Clusters. Geophysical Research Letters, 2019, 46, 10219-10229.	4.0	9
25	Very Low Latitude Whistlerâ€Mode Signals: Observations at Three Widely Spaced Latitudes. Journal of Geophysical Research: Space Physics, 2019, 124, 9253-9269.	2.4	Ο
26	What Fraction of the Outer Radiation Belt Relativistic Electron Flux at L â‰^ 3â€4.5 Was Lost to the Atmosphere During the Dropout Event of the St. Patrick's Day Storm of 2015?. Journal of Geophysical Research: Space Physics, 2019, 124, 9537-9551.	2.4	4
27	Characteristics of Relativistic Microburst Intensity From SAMPEX Observations. Journal of Geophysical Research: Space Physics, 2019, 124, 5627-5640.	2.4	20
28	Dâ€Region High‣atitude Forcing Factors. Journal of Geophysical Research: Space Physics, 2019, 124, 765-781.	2.4	7
29	Effects of VLF Transmitter Waves on the Inner Belt and Slot Region. Journal of Geophysical Research: Space Physics, 2019, 124, 5260-5277.	2.4	33
30	An Investigation of VLF Transmitter Wave Power in the Inner Radiation Belt and Slot Region. Journal of Geophysical Research: Space Physics, 2019, 124, 5246-5259.	2.4	40
31	The Source Regions of Whistlers. Journal of Geophysical Research: Space Physics, 2019, 124, 5082-5096.	2.4	7
32	The Effect of Ozone Shadowing on the <i>D</i> Region Ionosphere During Sunrise. Journal of Geophysical Research: Space Physics, 2019, 124, 3729-3742.	2.4	3
33	Groundâ€Based Observations of VLF Waves as a Proxy for Satellite Observations: Development of Models Including the Influence of Solar Illumination and Geomagnetic Disturbance Levels. Journal of Geophysical Research: Space Physics, 2019, 124, 2682-2696.	2.4	5
34	Simulation study for ground-based Ku-band microwave observations of ozone and hydroxyl in the polar middle atmosphere. Atmospheric Measurement Techniques, 2019, 12, 1375-1392.	3.1	4
35	Demonstrating the Use of a Class of Minâ€Max Smoothers for <i>D</i> Region Event Detection in Narrow Band VLF Phase. Radio Science, 2019, 54, 233-244.	1.6	7
36	Comparison of Multiple and Logistic Regression Analyses of Relativistic Electron Flux Enhancement at Geosynchronous Orbit Following Storms. Journal of Geophysical Research: Space Physics, 2019, 124, 10246-10256.	2.4	4

#	Article	IF	CITATIONS
37	Developing a Nowcasting Capability for Xâ€Class Solar Flares Using VLF Radiowave Propagation Changes Space Weather, 2019, 17, 1783-1799.	3.7	12
38	Comparison of Relativistic Microburst Activity Seen by SAMPEX With Groundâ€Based Wave Measurements at Halley, Antarctica. Journal of Geophysical Research: Space Physics, 2018, 123, 1279-1294.	2.4	15
39	Northern Hemisphere Stratospheric Ozone Depletion Caused by Solar Proton Events: The Role of the Polar Vortex. Geophysical Research Letters, 2018, 45, 2115-2124.	4.0	13
40	Polar Ozone Response to Energetic Particle Precipitation Over Decadal Time Scales: The Role of Mediumâ€Energy Electrons. Journal of Geophysical Research D: Atmospheres, 2018, 123, 607-622.	3.3	38
41	The Role of Localized Compressional Ultraâ€low Frequency Waves in Energetic Electron Precipitation. Journal of Geophysical Research: Space Physics, 2018, 123, 1900-1914.	2.4	36
42	Mesospheric Nitric Acid Enhancements During Energetic Electron Precipitation Events Simulated by WACCMâ€Ð. Journal of Geophysical Research D: Atmospheres, 2018, 123, 6984-6998.	3.3	12
43	An Updated Model Providing Longâ€Term Data Sets of Energetic Electron Precipitation, Including Zonal Dependence. Journal of Geophysical Research D: Atmospheres, 2018, 123, 9891-9915.	3.3	37
44	Quiet Daytime Arctic IonosphericDRegion. Journal of Geophysical Research: Space Physics, 2018, 123, 9726-9742.	2.4	6
45	A Distributed Lag Autoregressive Model of Geostationary Relativistic Electron Fluxes: Comparing the Influences of Waves, Seed and Source Electrons, and Solar Wind Inputs. Journal of Geophysical Research: Space Physics, 2018, 123, 3646-3671.	2.4	20
46	Observations and Modeling of Increased Nitric Oxide in the Antarctic Polar Middle Atmosphere Associated With Geomagnetic Stormâ€Đriven Energetic Electron Precipitation. Journal of Geophysical Research: Space Physics, 2018, 123, 6009-6025.	2.4	22
47	Nonlinear and Synergistic Effects of ULF Pc5, VLF Chorus, and EMIC Waves on Relativistic Electron Flux at Geosynchronous Orbit. Journal of Geophysical Research: Space Physics, 2018, 123, 4755-4766.	2.4	21
48	Relativistic Electron Microburst Events: Modeling the Atmospheric Impact. Geophysical Research Letters, 2018, 45, 1141-1147.	4.0	23
49	Long‣asting Geomagnetically Induced Currents and Harmonic Distortion Observed in New Zealand During the 7–8 September 2017 Disturbed Period. Space Weather, 2018, 16, 704-717.	3.7	48
50	Investigating energetic electron precipitation through combining groundâ€based and balloon observations. Journal of Geophysical Research: Space Physics, 2017, 122, 534-546.	2.4	31
51	Evidence of subâ€MeV EMICâ€driven electron precipitation. Geophysical Research Letters, 2017, 44, 1210-1218.	4.0	66
52	Energetic electron precipitation and auroral morphology at the substorm recovery phase. Journal of Geophysical Research: Space Physics, 2017, 122, 6508-6527.	2.4	20
53	Longâ€Term Geomagnetically Induced Current Observations From New Zealand: Peak Current Estimates for Extreme Geomagnetic Storms. Space Weather, 2017, 15, 1447-1460.	3.7	44
54	Longâ€ŧerm geomagnetically induced current observations in New Zealand: Earth return corrections and geomagnetic field driver. Space Weather, 2017, 15, 1020-1038.	3.7	43

#	Article	IF	CITATIONS
55	Occurrence characteristics of relativistic electron microbursts from SAMPEX observations. Journal of Geophysical Research: Space Physics, 2017, 122, 8096-8107.	2.4	37
56	Midlatitude ionospheric <i>D</i> region: Height, sharpness, and solar zenith angle. Journal of Geophysical Research: Space Physics, 2017, 122, 8933-8946.	2.4	19
57	Long-term climate change in the D-region. Scientific Reports, 2017, 7, 16683.	3.3	8
58	Solar forcing for CMIP6 (v3.2). Geoscientific Model Development, 2017, 10, 2247-2302.	3.6	293
59	<i>D</i> -region ion–neutral coupled chemistry (Sodankyläon Chemistry,) Tj ET WACCM-rSIC. Geoscientific Model Development, 2016, 9, 3123-3136.	Qq1 1 0.7 3.6	784314 rgB 16
60	A model providing longâ€ŧerm data sets of energetic electron precipitation during geomagnetic storms. Journal of Geophysical Research D: Atmospheres, 2016, 121, 12,520.	3.3	63
61	Nature's Grand Experiment: Linkage between magnetospheric convection and the radiation belts. Journal of Geophysical Research: Space Physics, 2016, 121, 171-189.	2.4	42
62	Confirmation of EMIC waveâ€driven relativistic electron precipitation. Journal of Geophysical Research: Space Physics, 2016, 121, 5366-5383.	2.4	43
63	Empirical predictive models of daily relativistic electron flux at geostationary orbit: Multiple regression analysis. Journal of Geophysical Research: Space Physics, 2016, 121, 3181-3197.	2.4	34
64	Linkages Between the Radiation Belts, Polar Atmosphere and Climate: Electron Precipitation Through Wave Particle Interactions. , 2016, , 354-376.		9
65	Substormâ€induced energetic electron precipitation: Impact on atmospheric chemistry. Geophysical Research Letters, 2015, 42, 8172-8176.	4.0	51
66	Highâ€resolution in situ observations of electron precipitationâ€causing EMIC waves. Geophysical Research Letters, 2015, 42, 9633-9641.	4.0	59
67	A case study of electron precipitation fluxes due to plasmaspheric hiss. Journal of Geophysical Research: Space Physics, 2015, 120, 6736-6748.	2.4	13
68	Observations of coincident EMIC wave activity and duskside energetic electron precipitation on 18–19 January 2013. Geophysical Research Letters, 2015, 42, 5727-5735.	4.0	102
69	Electron precipitation from EMIC waves: A case study from 31 May 2013. Journal of Geophysical Research: Space Physics, 2015, 120, 3618-3631.	2.4	65
70	Analysis of the effectiveness of groundâ€based VLF wave observations for predicting or nowcasting relativistic electron flux at geostationary orbit. Journal of Geophysical Research: Space Physics, 2015, 120, 2052-2060.	2.4	12
71	Longâ€ŧerm determination of energetic electron precipitation into the atmosphere from AARDDVARK subionospheric VLF observations. Journal of Geophysical Research: Space Physics, 2015, 120, 2194-2211.	2.4	29
72	Substormâ€induced energetic electron precipitation: Morphology and prediction. Journal of Geophysical Research: Space Physics, 2015, 120, 2993-3008.	2.4	34

#	Article	IF	CITATIONS
73	Energetic electron precipitation associated with pulsating aurora: EISCAT and Van Allen Probe observations. Journal of Geophysical Research: Space Physics, 2015, 120, 2754-2766.	2.4	133
74	Techniques to determine the quiet day curve for a long period of subionospheric VLF observations. Radio Science, 2015, 50, 453-468.	1.6	9
75	First optical observations of energetic electron precipitation at 4278 Ã caused by a powerful VLF transmitter. Geophysical Research Letters, 2014, 41, 2237-2242.	4.0	2
76	Energetic particle forcing of the Northern Hemisphere winter stratosphere: comparison to solar irradiance forcing. Frontiers in Physics, 2014, 2, .	2.1	27
77	Detecting space weather events with subionospheric VLF observations: Producing quiet day curves from AARDDVARK data. , 2014, , .		1
78	Missing driver in the Sun–Earth connection from energetic electron precipitation impacts mesospheric ozone. Nature Communications, 2014, 5, 5197.	12.8	148
79	Prediction of relativistic electron flux at geostationary orbit following storms: Multiple regression analysis. Journal of Geophysical Research: Space Physics, 2014, 119, 7297-7318.	2.4	35
80	Lowâ€latitude ionospheric <i>D</i> region dependence on solar zenith angle. Journal of Geophysical Research: Space Physics, 2014, 119, 6865-6875.	2.4	24
81	A statistical approach to determining energetic outer radiation belt electron precipitation fluxes. Journal of Geophysical Research: Space Physics, 2014, 119, 3961-3978.	2.4	11
82	The effects and correction of the geometric factor for the POES/MEPED electron flux instrument using a multisatellite comparison. Journal of Geophysical Research: Space Physics, 2014, 119, 6386-6404.	2.4	17
83	Characteristics of precipitating energetic electron fluxes relative to the plasmapause during geomagnetic storms. Journal of Geophysical Research: Space Physics, 2014, 119, 8784-8800.	2.4	16
84	Longitudinal hotspots in the mesospheric OH variations due to energetic electron precipitation. Atmospheric Chemistry and Physics, 2014, 14, 1095-1105.	4.9	40
85	Long term determination of variations in energetic electron precipitation into the atmosphere using AARDDVARK. , 2014, , .		0
86	Geomagnetic activity signatures in wintertime stratosphere wind, temperature, and wave response. Journal of Geophysical Research D: Atmospheres, 2013, 118, 2169-2183.	3.3	95
87	Lower ionosphere monitoring by the South America VLF Network (SAVNET): <i>C</i> region occurrence and atmospheric temperature variability. Journal of Geophysical Research: Space Physics, 2013, 118, 6686-6693.	2.4	6
88	Rapid Radiation Belt Losses Occurring During High-Speed Solar Wind Stream-Driven Storms: Importance of Energetic Electron Precipitation. Geophysical Monograph Series, 2013, , 213-224.	0.1	21
89	The Balloon Array for RBSP Relativistic Electron Losses (BARREL). Space Science Reviews, 2013, 179, 503-530.	8.1	76
90	POES satellite observations of EMICâ€wave driven relativistic electron precipitation during 1998–2010. Journal of Geophysical Research: Space Physics, 2013, 118, 232-243.	2.4	87

#	Article	IF	CITATIONS
91	A reexamination of latitudinal limits of substormâ€produced energetic electron precipitation. Journal of Geophysical Research: Space Physics, 2013, 118, 6694-6705.	2.4	28
92	Energetic electron precipitation characteristics observed from Antarctica during a flux dropout event. Journal of Geophysical Research: Space Physics, 2013, 118, 6921-6935.	2.4	9
93	The plasmasphere during a space weather event: first results from the PLASMON project. Journal of Space Weather and Space Climate, 2013, 3, A23.	3.3	50
94	Determining the spectra of radiation belt electron losses: Fitting DEMETER electron flux observations for typical and storm times. Journal of Geophysical Research: Space Physics, 2013, 118, 7611-7623.	2.4	41
95	Observations of nitric oxide in the Antarctic middle atmosphere during recurrent geomagnetic storms. Journal of Geophysical Research: Space Physics, 2013, 118, 7874-7885.	2.4	9
96	Comparison between POES energetic electron precipitation observations and riometer absorptions: Implications for determining true precipitation fluxes. Journal of Geophysical Research: Space Physics, 2013, 118, 7810-7821.	2.4	63
97	Simultaneous observation of chorus and hiss near the plasmapause. Journal of Geophysical Research, 2012, 117, .	3.3	12
98	Tropical daytime lower Dâ€region dependence on sunspot number. Journal of Geophysical Research, 2012, 117, .	3.3	5
99	Combined THEMIS and groundâ€based observations of a pair of substormâ€associated electron precipitation events. Journal of Geophysical Research, 2012, 117, .	3.3	13
100	The annual and longitudinal variations in plasmaspheric ion density. Journal of Geophysical Research, 2012, 117, .	3.3	16
101	Trend and abrupt changes in longâ€ŧerm geomagnetic indices. Journal of Geophysical Research, 2012, 117, ·	3.3	7
102	Precipitating radiation belt electrons and enhancements of mesospheric hydroxyl during 2004–2009. Journal of Geophysical Research, 2012, 117, .	3.3	54
103	Energetic particle injection, acceleration, and loss during the geomagnetic disturbances which upset Galaxy 15. Journal of Geophysical Research, 2012, 117, .	3.3	28
104	Contrasting the responses of three different groundâ€based instruments to energetic electron precipitation. Radio Science, 2012, 47, .	1.6	53
105	Source region for whistlers detected at Rothera, Antarctica. Journal of Geophysical Research, 2011, 116, .	3.3	22
106	First evidence of mesospheric hydroxyl response to electron precipitation from the radiation belts. Journal of Geophysical Research, 2011, 116, .	3.3	75
107	Direct observations of nitric oxide produced by energetic electron precipitation into the Antarctic middle atmosphere. Geophysical Research Letters, 2011, 38, n/a-n/a.	4.0	38
108	Daytime <i>D</i> region parameters from long-path VLF phase and amplitude. Journal of Geophysical Research, 2011, 116, n/a-n/a.	3.3	15

#	Article	IF	CITATIONS
109	Daytime midlatitude <i>D</i> region parameters at solar minimum from short-path VLF phase and amplitude. Journal of Geophysical Research, 2011, 116, .	3.3	45
110	Geomagnetic activity related NO _x enhancements and polar surface air temperature variability in a chemistry climate model: modulation of the NAM index. Atmospheric Chemistry and Physics, 2011, 11, 4521-4531.	4.9	118
111	Unusual observation of chorus at L=2.6. , 2011, , .		0
112	Energetic outer radiation belt electron precipitation during recurrent solar activity. Journal of Geophysical Research, 2010, 115, .	3.3	15
113	High-latitude geomagnetically induced current events observed on very low frequency radio wave receiver systems. Radio Science, 2010, 45, n/a-n/a.	1.6	5
114	Radiation belt electron precipitation due to geomagnetic storms: Significance to middle atmosphere ozone chemistry. Journal of Geophysical Research, 2010, 115, .	3.3	31
115	Groundâ€based estimates of outer radiation belt energetic electron precipitation fluxes into the atmosphere. Journal of Geophysical Research, 2010, 115, .	3.3	50
116	Contrasting the efficiency of radiation belt losses caused by ducted and nonducted whistlerâ€mode waves from groundâ€based transmitters. Journal of Geophysical Research, 2010, 115, .	3.3	79
117	Automatic Whistler Detector and Analyzer system: Implementation of the analyzer algorithm. Journal of Geophysical Research, 2010, 115, .	3.3	16
118	Relativistic microburst storm characteristics: Combined satellite and groundâ€based observations. Journal of Geophysical Research, 2010, 115, .	3.3	27
119	Use of POES SEMâ€2 observations to examine radiation belt dynamics and energetic electron precipitation into the atmosphere. Journal of Geophysical Research, 2010, 115, .	3.3	209
120	Impact of different energies of precipitating particles on NOx generation in the middle and upper atmosphere during geomagnetic storms. Journal of Atmospheric and Solar-Terrestrial Physics, 2009, 71, 1176-1189.	1.6	166
121	Remote sensing space weather events: Antarcticâ€Arctic Radiationâ€belt (Dynamic) Depositionâ€VLF Atmospheric Research Konsortium network. Space Weather, 2009, 7, .	3.7	102
122	Additional stratospheric NO _{<i>x</i>} production by relativistic electron precipitation during the 2004 spring NO _{<i>x</i>} descent event. Journal of Geophysical Research, 2009, 114, .	3.3	29
123	Geomagnetic activity and polar surface air temperature variability. Journal of Geophysical Research, 2009, 114, .	3.3	135
124	Hiss from the chorus. Nature, 2008, 452, 41-42.	27.8	13
125	Groundâ€based transmitter signals observed from space: Ducted or nonducted?. Journal of Geophysical Research, 2008, 113, .	3.3	60
126	Geomagnetic perturbations on stratospheric circulation in late winter and spring. Journal of Geophysical Research, 2008, 113, .	3.3	49

#	Article	IF	CITATIONS
127	Significance of transient luminous events to neutral chemistry: Experimental measurements. Geophysical Research Letters, 2008, 35, .	4.0	31
128	Observations of relativistic electron precipitation from the radiation belts driven by EMIC waves. Geophysical Research Letters, 2008, 35, .	4.0	93
129	Energetic electron precipitation during substorm injection events: Highâ€latitude fluxes and an unexpected midlatitude signature. Journal of Geophysical Research, 2008, 113, .	3.3	39
130	Radiation belt electron precipitation by manâ€made VLF transmissions. Journal of Geophysical Research, 2008, 113, .	3.3	73
131	The effects of hardâ€spectra solar proton events on the middle atmosphere. Journal of Geophysical Research, 2008, 113, .	3.3	47
132	Atmospheric impact of the Carrington event solar protons. Journal of Geophysical Research, 2008, 113,	3.3	25
133	World-wide lightning location using VLF propagation in the Earth-ionosphere waveguide. IEEE Antennas and Propagation Magazine, 2008, 50, 40-60.	1.4	65
134	Temporal variability of the descent of highâ€altitude NO _X inferred from ionospheric data. Journal of Geophysical Research, 2007, 112, .	3.3	26
135	NO _x enhancements in the middle atmosphere during 2003–2004 polar winter: Relative significance of solar proton events and the aurora as a source. Journal of Geophysical Research, 2007, 112, .	3.3	45
136	Arctic and Antarctic polar winter NOxand energetic particle precipitation in 2002–2006. Geophysical Research Letters, 2007, 34, .	4.0	97
137	Nighttime ionospheric <i>D</i> region parameters from VLF phase and amplitude. Journal of Geophysical Research, 2007, 112, .	3.3	87
138	Storm time, shortâ€lived bursts of relativistic electron precipitation detected by subionospheric radio wave propagation. Journal of Geophysical Research, 2007, 112, .	3.3	22
139	Radiation belt electron precipitation into the atmosphere: Recovery from a geomagnetic storm. Journal of Geophysical Research, 2007, 112, .	3.3	75
140	Energetic particle precipitation into the middle atmosphere triggered by a coronal mass ejection. Journal of Geophysical Research, 2007, 112, .	3.3	33
141	Improved dynamic geomagnetic rigidity cutoff modeling: Testing predictive accuracy. Journal of Geophysical Research, 2007, 112, .	3.3	12
142	Longitudinal and seasonal variations in plasmaspheric electron density: Implications for electron precipitation. Journal of Geophysical Research, 2007, 112, .	3.3	24
143	Lightning-driven inner radiation belt energy deposition into the atmosphere: implications for ionisation-levels and neutral chemistry. Annales Geophysicae, 2007, 25, 1745-1757.	1.6	25
144	The importance of atmospheric precipitation in storm-time relativistic electron flux drop outs. Geophysical Research Letters, 2006, 33, n/a-n/a.	4.0	35

#	Article	IF	CITATIONS
145	Destruction of the tertiary ozone maximum during a solar proton event. Geophysical Research Letters, 2006, 33, .	4.0	75
146	Dynamic geomagnetic rigidity cutoff variations during a solar proton event. Journal of Geophysical Research, 2006, 111, .	3.3	43
147	Modeling polar ionospheric effects during the October-November 2003 solar proton events. Radio Science, 2006, 41, n/a-n/a.	1.6	32
148	Predicting Solar Cycle 24 and beyond. Space Weather, 2006, 4, n/a-n/a.	3.7	46
149	Ionospheric evidence of thermosphere-to-stratosphere descent of polar NOX. Geophysical Research Letters, 2006, 33, .	4.0	39
150	Origins of plasmaspheric hiss. Journal of Geophysical Research, 2006, 111, .	3.3	118
151	The atmospheric implications of radiation belt remediation. Annales Geophysicae, 2006, 24, 2025-2041.	1.6	20
152	Lightning driven inner radiation belt energy deposition into the atmosphere: regional and global estimates. Annales Geophysicae, 2005, 23, 3419-3430.	1.6	13
153	Large solar flares and their ionosphericDregion enhancements. Journal of Geophysical Research, 2005, 110, .	3.3	131
154	Reconstructing the long-termaaindex. Journal of Geophysical Research, 2005, 110, .	3.3	39
155	Modeling a large solar proton event in the southern polar atmosphere. Journal of Geophysical Research, 2005, 110, .	3.3	41
156	Diurnal variation of ozone depletion during the October-November 2003 solar proton events. Journal of Geophysical Research, 2005, 110, .	3.3	147
157	Polar mesosphere summer echo detection using a dynasonde. Radio Science, 2005, 40, n/a-n/a.	1.6	0
158	Testing the importance of precipitation loss mechanisms in the inner radiation belt. Geophysical Research Letters, 2004, 31, n/a-n/a.	4.0	16
159	Radiation belt electron precipitation fluxes associated with lightning. Journal of Geophysical Research, 2004, 109, .	3.3	17
160	Investigating radiation belt losses though numerical modelling of precipitating fluxes. Annales Geophysicae, 2004, 22, 3657-3667.	1.6	9
161	Solar activity levels in 2100. Astronomy and Geophysics, 2003, 44, 5.20-5.22.	0.2	30
162	In situ and ground-based intercalibration measurements of plasma density atL= 2.5. Journal of Geophysical Research, 2003, 108, .	3.3	24

#	Article	IF	CITATIONS
163	Significance of lightning-generated whistlers to inner radiation belt electron lifetimes. Journal of Geophysical Research, 2003, 108, .	3.3	53
164	Inner radiation belt electron lifetimes due to whistler-induced electron precipitation (WEP) driven losses. Geophysical Research Letters, 2002, 29, 30-1-30-4.	4.0	17
165	Determining the size of lightning-induced electron precipitation patches. Journal of Geophysical Research, 2002, 107, SIA 10-1-SIA 10-11.	3.3	32
166	Dregion reflection height modification by whistler-induced electron precipitation. Journal of Geophysical Research, 2002, 107, SIA 18-1.	3.3	10
167	The causes of long-term change in theaaindex. Journal of Geophysical Research, 2002, 107, SSH 4-1-SSH 4-7.	3.3	33
168	Total solar eclipse effects on VLF signals: Observations and modeling. Radio Science, 2001, 36, 773-788.	1.6	86
169	Solar flare induced ionospheric D-region enhancements from VLF amplitude observations. Journal of Atmospheric and Solar-Terrestrial Physics, 2001, 63, 1729-1737.	1.6	106
170	Plasmaspheric storm time erosion. Journal of Geophysical Research, 2000, 105, 12997-13008.	3.3	22
171	Solar cycle changes in daytime VLF subionospheric attenuation. Journal of Atmospheric and Solar-Terrestrial Physics, 2000, 62, 601-608.	1.6	40
172	The effect of snow accumulation on imaging riometer performance. Radio Science, 2000, 35, 1143-1153.	1.6	7
173	Latitudinally dependent Trimpi effects: Modeling and observations. Journal of Geophysical Research, 1999, 104, 19881-19887.	3.3	18
174	Monitoring spatial and temporal variations in the dayside plasmasphere using geomagnetic field line resonances. Journal of Geophysical Research, 1999, 104, 19955-19969.	3.3	100
175	Sunrise effects on VLF signals propagating over a long north-south path. Radio Science, 1999, 34, 939-948.	1.6	62
176	Ground-based evidence of latitude-dependent cyclotron absorption of whistler mode signals originating from VLF transmitters. Journal of Geophysical Research, 1996, 101, 2355-2367.	3.3	20
177	Characteristics of localized ionospheric disturbances inferred from VLF measurements at two closely spaced receivers. Journal of Geophysical Research, 1996, 101, 15737-15747.	3.3	15
178	Monitoring space weather: using automated, accurate neural network based whistler segmentation for whistler inversion. Space Weather, 0, , .	3.7	0